

Fuzzy Adaptive Control of an Induction Motor Drive

UDK 621.313.333.07
IFAC IA 2.1.4;3.1.1

Original scientific paper

Industrial applications increasingly require electric drives with good position command tracking and load regulation responses. These conditions can only be achieved by adaptive-type control because of the loading conditions, inertias and system parameters all change during the motion.

For this paper an Adaptive Speed Controller for AC drives with a very low computational algorithm was developed. The authors propose self-tuning control based on a supervisory fuzzy adaptation. The supervisor continuously monitors the status of the system and changes the K_f parameter of a standard PDF controller to adapt it to the plant's evolution.

The fuzzy logic adaptive strategy was readily implemented and showed very fast learning features and very good tracking and regulation characteristics. The stability of the controller developed was also analysed, and experimental results demonstrated the robustness of the suggested algorithm in contending with varying load and torque disturbance.

Key words: adaptive control, adjustable speed drives, fuzzy logic, motion control, variable speed drives

1 INTRODUCTION

Conventional proportional-plus-integral (PI) regulators have perhaps been the most widely used control method for the speed loop in high-performance AC inverter drives. However, other types of simple one-degree-of-freedom controllers such as PDF (Pseudo-Derivative-Feedback) control, have been also used [1].

The proportional term of the PDF controller uses the speed output directly when applied to motion control systems. This structure makes PDF control less responsive to the reference than the PI controller, but allows closed-loop poles of the transfer function be properly placed, thus improving load torque-disturbance rejection capability. The PDF controller is one of the best options for closing the speed loop, providing both satisfactory disturbance rejection and suitable tracking performance in the drive, which are the most important design criteria in motion control systems.

Nevertheless, conventional controllers, such as the PDF controllers, require a mathematical model that represents the system under control [2], which is a major limiting factor for systems whose varying dynamics are unknown. For advanced drives, for which the objectives are to achieve both good position command tracking and load regulation, the performance is still not satisfactory under wide operating ranges if the controller parameters are not adaptively tuned according to the variations of the

drive parameters. Tracking and regulation accuracy must not be affected by parameter uncertainties, unknown load variations or external disturbances, and this can only be achieved by adaptive-type control because the loading conditions, inertias and system parameters all change during motion.

Adaptive regulators, which take both tracking and regulations capabilities into account and are able to modify their features in order to maintain the desired behaviour of the system, are increasingly being used [3, 4].

Over the years, such adaptive speed-control systems have fallen into one of two categories: model reference adaptive control (MRAC) or self-tuning regulators (STR). Self-tuning regulator controllers for motion control that use recursive methods to estimate the parameters of the system have been the most frequent subject of recent analysis in the field [5, 6]. Unfortunately, the complexity of these algorithms is a significant obstacle to the microprocessors used in low- and medium-cost motor drives.

Other authors have used fuzzy logic to construct self-tuning non-linear controllers. Robust controllers whose structures are changed continuously by fuzzy logic, depending on the error speed and its time derivative, are presented in [7] and [8]. However, the stability of the whole system is only demonstrated in the continuous s space, neglecting both the current-control loop-time constant and the control digitization.

As an alternative, this paper proposes a single and efficient self-tuning speed control that does not use a recursive estimator or observers, but is instead based on a supervisory fuzzy adaptation. The supervisor continuously monitors the status of the system and changes the K_i parameter of a standard PDF controller in order to adapt it to the plant's evolution according to the dynamics of the system.

The adaptive supervision takes place in two stages. The base control changes K_i parameter depending on the speed error amplitude and the auxiliary part drives current K_i value by increasing or decreasing it on a step-by-step basis if error control degrades.

The speed regulator was applied to a vector torque control driving a non-linear load, and the whole system was verified by computer simulation. Taking into account control delays and digitization, the asymptotic stability of the adaptive algorithm in a Lyapunov's sense was demonstrated. Experimental results also confirmed the effectiveness of the suggested regulator.

2 SYSTEM CONTROL DESCRIPTION

The motion control algorithm shown in Figure 1 is based on the mechatronics assumption of an almost ideal, field-oriented torque controller in a cascade control topology. If it is assumed that proper torque control with high-gain, closed-loop current control was implemented, then the complex dynamics of AC motor torque control can be substituted by a λ delay when modeling the drive and performing simulations.

The dynamic model of the mechanical system can be expressed as

$$J \frac{d\omega}{dt} + B\omega + \Gamma_L = \Gamma, \tag{1}$$

$$\Gamma_L = K_0 + K_1\omega + K_2\omega^2 \tag{2}$$

Table 1 Parameters of the plant

Parameter	Nominal value	Limit values
J , kg · m ²	$J_{nom} = 0.016$	$J_{nom}/5 < J < 5 J_{nom}$
K_0 , N · m	$K_{0\ nom} = 1.6$	$0 \leq K_0 < 3 K_{0\ nom}$
K_1 , N · ms/rad	$K_{1\ nom} = 0.03$	$0 \leq K_1 < 3 K_{1\ nom}$
K_2 , N · m s ² /rad ²	$K_{2\ nom} = 0.00005$	$K_{2\ nom}/3 < K_2 < 3 K_{2\ nom}$
ω_m^* , rad/s	$\omega_{m\ nom} = 148$	$-4 \omega_{m\ nom} < \omega_m < 4 \omega_{m\ nom}$
λ , μ s	$\lambda_{nom} = 400$	$\lambda_{nom}/3 < \lambda < 3 \lambda_{nom}$
B , N · ms/rad	$B_{nom} = 0.0015$	constant value

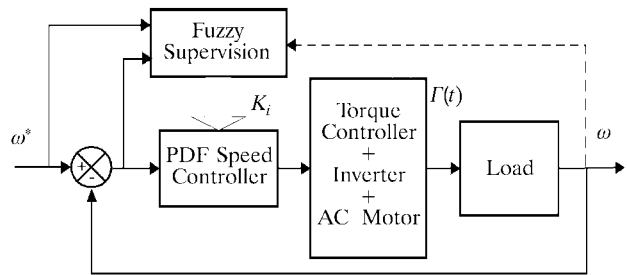


Fig. 1 Functional block diagram of proposed self-tuning adaptive controller

where J and B denote the total inertia and viscous friction coefficient of the motor, ω is the rotor speed, and Γ and Γ_L are mechanical motor torque and disturbance load torque (2) respectively. K_0 , K_1 and K_2 are the coefficients of the Coulomb friction, the viscous friction of the load and the drag force due to turbulent air flow. Table 1 shows the parameters of the plant, which represent a realistic assumption for motor drives.

2.1 Speed Controller

Although the most popular controller for speed control in electrical drives is the classical PI controller, due to its easy implementation and tuning and its suitability, we chose the more sophisticated PDF algorithm, whose time-domain expression is as follows:

$$\Gamma^* = K_i \int (\omega^* - \omega) dt - K_p \omega \tag{3}$$

where K_i and K_p are the integral constant and the proportional gain respectively, and $(\omega^* - \omega)$ the speed error $e(t)$. In this design, the proportional gain acts only in the feedback path, thus preventing sudden changes in the speed command going directly to the actuator. In general, PDF controllers provide poorer command-tracking responses than PI controller, but improved disturbance rejection capability [9].

In motor control drives, it is often necessary to provide fast dynamics, which means that the speed controller is often saturated or close to saturation. However, when error decreases the output remains saturated due to integral term, which leads to a large overshoot and a large settling time of the process output. The most common anti-saturation techniques for speed controllers are anti-windup techniques. An anti-windup algorithm was included in the controller, whose final form in s space is shown in Figure 2. K_f is denoted as the tracking time constant, which was set to $K_f=K_i/2$ following the general rule $K_i/4 \leq K_f \leq K_i$.

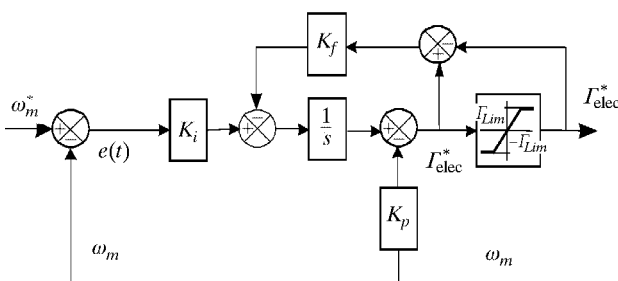


Fig. 2 Speed IP regulator with anti-wind-up technique implementation

2.2 System tuning considerations

The basic characteristic of the transient response of a closed-loop system is closely related to the location of the closed-loop poles, which are the roots of the characteristic equation. Thus, if this equation is known, poles can be located to force the system response is desired.

Despite the fact that the system being analysed is highly complex, several assumptions can be made that help to tune it. Assuming that torque control is perfectly tuned with motor parameters, and current regulations are well implemented, the complex dynamics of ac motor will simplify to a simple torque-commanded model. Moreover, in analysis the response of the outer loop, the inner torque loop can only be considered a delay. Thus, considering λ as the propagation time from the output of the speed controller to the input of the mechanical system, the dynamic model of the rotor speed (1) becomes

$$\Gamma(t-\lambda) - \Gamma_L = J \frac{d\omega}{dt} + B\omega. \quad (4)$$

By applying Taylor's formulae to $\Gamma(t-\lambda)$ in (4), deriving the speed and considering linear approximation of the system by letting $K_p \geq 10$ ($2 K_2 \omega$) ($K_p \geq 1.89$ is large enough to be considered as linear even the worst case), the Laplace transform of the

closed loop $\omega(t)/\omega^*(t)$, without considering zero-order hold or saturations in order to facilitate the design, is the following:

$$H(s) = \frac{\omega(s)}{\omega^*(s)} = \frac{K_i}{(J - \lambda K_p)s^2 + (K_1 + K_p - \lambda K_i)s + K_i}. \quad (5)$$

The closed-loop (5) is a typical second-order transfer function, in which the gain and closed-loop poles are as follows:

$$K = \frac{K_i}{J - \lambda K_p}$$

$$s = -\frac{K_1 + K_p - \lambda K_i}{2(J - \lambda K_p)} \pm \sqrt{\left(\frac{K_1 + K_p - \lambda K_i}{2(J - \lambda K_p)}\right)^2 - \frac{K_i}{J - \lambda K_p}}. \quad (6)$$

The dynamic behaviour of this system can be described in terms of two parameters, ζ and ω_n , which are the dumping ratio of the system and the undamped natural frequency

$$\zeta = \frac{K_1 + K_p - \lambda K_i}{2\sqrt{(J - \lambda K_p)K_i}};$$

$$\omega_n^2 = \frac{K_i}{J - \lambda K_p}. \quad (7)$$

As is well known, to avoid oscillatory response the following condition must be fulfilled: $\zeta \geq 1$. After operating in (7), this may be written approximately as follows:

$$K_p \geq -[K_1 + \lambda K_i] + 2\sqrt{(J + \lambda K_1)K_i}$$

$$K_i \geq \frac{2J - \lambda K_p - 2\sqrt{J^2 - J\lambda K_p}}{\lambda^2} \quad (8)$$

which gives the relationship between the parameters of the PDF controller. Of the damping ratio values that respond without oscillations, the critically damped response is the fastest. Moreover, the closer the damping ratio is to 1, the lower the overshoot.

In spite of the fact that the analysis above cannot be carried out when saturations are considered, it does provide general rules for tuning the system. Thus, the rise time of the system, defined as the time required for the response to rise from 10 % to 90 %, decreases when the value of ω_n is high. Hence, the value of K_i should be high if fast tracking is desired (9). Furthermore, high values of K_i lead to low ramp-tracking errors.

However, to limit the maximum overshoot, the dumping ratio ζ should not be too small; in this case, expression (8) have to be considered.

$$t_r = \frac{1}{\omega_n \left(\sqrt{1-\zeta^2} \right)} \tan^{-1} \left(-\frac{\sqrt{1-\zeta^2}}{\zeta} \right) \quad (9)$$

The discussion above yields the conclusion that K_i and K_p must be as higher as possible to improve the response of the system under all conditions. However, if saturation nonlinearity is considered, sustained oscillations may appear for a sufficiently high system gain $K_g = K_i / (J - \lambda K_p)$. Since gain K_g directly depends on K_i , we conclude that the parameters of the controller should not be too large if oscillations are to be avoided.

3 STABILITY ANALYSIS

Let us now consider zero-order hold in Figure 3, although not, at this stage, the saturation block, which will be introduced later. In discrete z-domain, the open-loop transfer function in Equation (5) becomes Equation (10) T being the sampling time of the zero-order hold. The closed-loop transfer function is Equation (11).

$$G_p(z) = K_c \left(\frac{ATz^{-1}}{1-z^{-1}} + B + \frac{C(1-z^{-1})}{(1-e^{-aTz})z^{-1}} \right)$$

$$K_c = \frac{K_i}{J - \lambda K_p}; \quad a = \frac{(K_1 + K_p - \lambda K_i)}{J - \lambda K_p} \quad (10)$$

$$A = \frac{1}{a}; \quad B = -C = \frac{1}{a^2}$$

$$G(z) = \frac{K_c \left[z^{-1}(AT - B(1 + e^{-aT}) - 2C) + z^{-2}(-AT + Be^{-aT} + C) \right]}{\left[1 - z^{-1}(1 + e^{-aT} - KAT + KBe^{-aT} + KC) + z^{-2}(e^{-aT} - KATe^{-aT} + KBe^{-aT} + KC) \right]} \quad (11)$$

which can be simplified as

$$G(z) = \frac{b_1 z^{-1} + b_2 z^{-2}}{1 - a_1 z^{-1} + a_2 z^{-2}}$$

To obtain state space representation, where $a_{12} = a_2$, $a_{22} = a_1$,

$$x_1(k+1) = -a_{12}x_2(k) + \beta_1 u(k)$$

$$x_2(k+1) = x_1(k) + a_{22}x_2(k) + \beta_2 u(k) \quad (12)$$

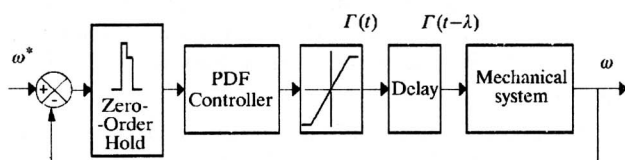


Fig. 3 System block diagram for stability analysis

Considering a time invariant system in which the origin at equilibrium is state-defined at the current input, then Equation (12) becomes $\chi(k+1) = A\chi(k)$, where $\chi = (\chi_1, \chi_2)$ is a real state vector and $A(a_{ij})$ is a real constant 2×2 matrix.

Let us choose a possible positive definite Lyapunov function $V(\chi(k)) = \chi^T(k) \cdot P\chi(k)$, where $P(p_{ij})$ is a positive definite Hermitian matrix. The time derivative of $V(\chi)$ along any trajectory is $\Delta V(\chi(k)) = V(\chi(k+1)) - V(\chi(k)) = \chi^T(k)[A^T P A - P]\chi(k)$.

For asymptotic stability,

$$\Delta V(\chi(k)) = -\chi^T(k) \cdot Q\chi(k),$$

where

$$Q = -(A^T P A - P)$$

must be positive definite.

A positive definite matrix Q is specified here, and then P is examined. If a positive definite Hermitian matrix P such that $A^T P A - P = -Q$ exists, then the system will be asymptotically stable at the equilibrium state.

Let us choose Q as positive definite unity matrix. It can be established that, for P to be positive definite, it is necessary and sufficient that

$$a_{22} < 1/\sqrt{2} (1+a_{12}) \quad (13)$$

$$a_{12} < 1. \quad (14)$$

From these conditions, it can be proved that, to ensure the system is asymptotically stable, it is necessary and sufficient condition that

$$0 < K_i < \frac{K_p + K_1}{T + \lambda}. \quad (15)$$

To analyse the stability under saturation Krasovskii's stability analysis procedure is used [10]. The dynamic model of the rotor speed thus becomes

$$\Gamma_{\text{sat}}(\lambda) = \Gamma_{\text{sat}}(t-\lambda) = \Gamma_{\text{sat}} = K_0 + K_1 \omega + K_2 \omega^2 + J \frac{d\omega}{dt}. \quad (16)$$

By defining new state variables as $\chi_1 = d\omega/dt$ and $\chi_2 = \omega$, the Hermitian matrix of the system

$$\hat{J}(\chi) = J^*(\chi) + J(\chi),$$

where $J^*(\chi)$ is the complex conjugate of the Jacobian $J(\chi)$, becomes

$$\hat{\mathbf{J}}(x) = \begin{bmatrix} 2 \frac{-K_1 - 2K_2\chi_2}{J} & 1 - \frac{2K_2\chi_1}{J} \\ 1 - \frac{2K_2\chi_1}{J} & 0 \end{bmatrix} \quad (17)$$

which is negative definite, as may be proved by analysing the successive principal minors. Then the equilibrium state $\chi = \mathbf{0}$ is asymptotically stable.

To conclude, the system presents instability when working in the linear zone if condition (17) is not fulfilled; a sustained oscillation that is small in amplitude may appear at the output when saturation is achieved.

4 SUPERVISORY FUZZY AND TUNING

In many motion control applications, plant parameters such as friction and load inertia are not fully ascertained until the final installation. Moreover, they may even vary widely during operation. Since a PDF controller is robust in low-perturbation situations but becomes under optimal when significant variations occur in the control loop parameters, the goal of the supervisor is to improve the controller so that it can achieve optimal performance in a highly perturbed and/or non-linear context.

The internal structure of the fuzzy supervisor is the same as that of the standard fuzzy controller, the input variables the performance values of the dynamical process (the speed error and its derivative), and the output variables the changes to be applied to the K_i parameter of the standard PDF controller. The relationship between input and output variables are established by means of fuzzy logic. The inference method is developed using Mamdani's standard minimum operation rule and the Centroid criterion (COG) is the defuzzification method.

In order to develop the supervisory system, some linguistic expressions must first be defined:

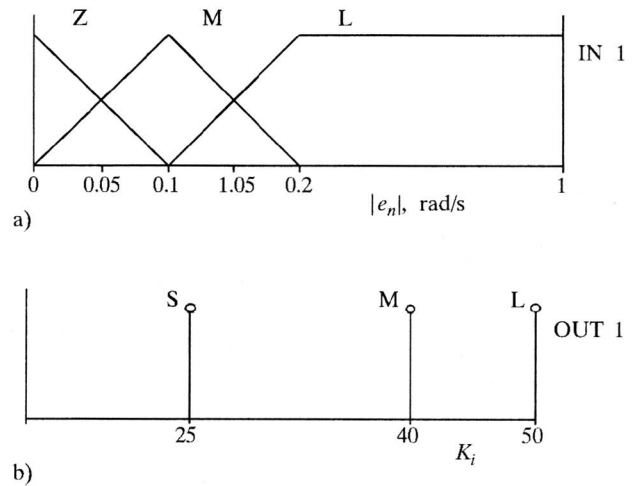


Fig. 5 Membership functions of the FL supervisor

- Since the integral term is responsible for the overshoot, the overshoot may be reduced by simply decreasing it when the error is large.
- The single integral effect of the Type I controller cannot lead to elimination of the ramp tracking error, which may be only reduced if K_i increases greatly.
- The plant's evolution must be tracked not only by means of the speed error but also by its evolution, i.e. by its derivative.

Figure 4 shows the supervisory fuzzy structure. One can see two parts: the main FLC that determines the base value of K_i , and the tracking block, which mainly engages this value according to speed error evolution.

Normalized inputs (18) are used, which simplifies the design of the membership functions, which are shown in Figure 5. According to experimental observations, the control strategy is as shown in (19).

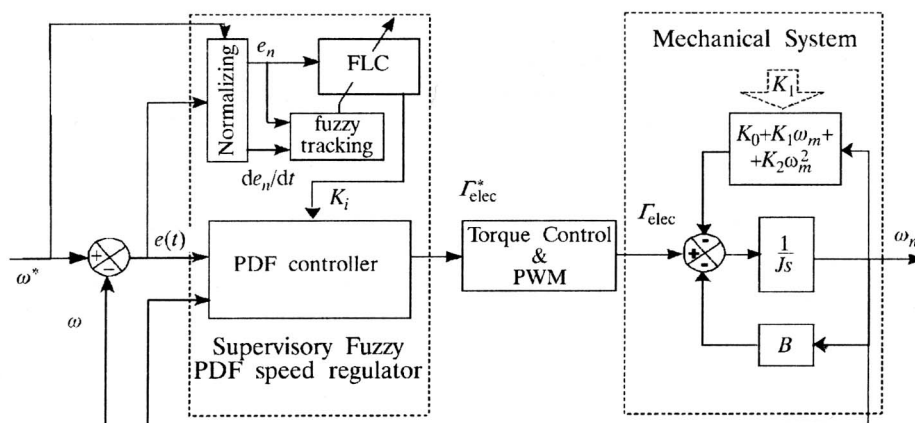


Fig. 4 Torque-controlled induction motor block diagram, including a supervisory fuzzy PDF speed control

$$e_n = \frac{e(t)}{\omega_m^*}; \quad |e_n| \quad (18)$$

$$e_n^* = \frac{de_n}{dt}; \quad |e_n^*|; \quad e_n^* \cdot e_n$$

- IF $|e_n|$ =Zero THEN K_i =Large
 IF $|e_n|$ =Medium THEN K_i =Medium (19)
 IF $|e_n|$ =Large THEN K_i =Small; $m = 3$

However, there are at least two situations in which FLC does not operate effectively, thus justifying the adaptive block:

- when the error is small and does not decrease but increases;
- when the error is close to zero and changes slowly or does not change, (i.e., ramp tracking).

The fuzzy supervisor was adapted to improve control behaviour under these conditions. A delta factor δ was increased and decreased step by step, which multiplied K_i value while the conditions described above persisted. Therefore, a reinforcement of the output action was introduced. The control of the delta factor depends on the value of one additional input, $e_n \dot{e}_n$, which relates to the control principle $e_n \dot{e}_n < 0$, and determines the evolution of the error (Figure 6).

Delta control also analyses the error evolution in relation to the error amplitude: if an error exists, but it does not change or does it slowly, the K_i value is also incremented by the δ factor. To avoid K_i correction when the error is being reduced correctly, delta adaptation will be disconnected if $|\dot{e}_n|$ is higher than fifty percent.

We also noted that derivative signal is obtained by computation. Generally, the derivative computation is sensitive to the unmodelled vibratory model and measurement noise. Therefore, a small first-order filter was added to the output of this adapter, whose pole does not restrict the system's frequency response band.

The fuzzy tracking block uses the same Mamdani fuzzy reasoning and centroid defuzzification approach as the main fuzzy block. The rules of this auxiliary system are as shown in (20). The block diagram of adaptation is shown in Figure 7.

- IF $|e_n|$ =Large AND $e_n \dot{e}_n$ =Negative THEN δ =Large
 IF $|e_n|$ =Medium AND $e_n \dot{e}_n$ =Negative THEN δ =Small
 IF $|e_n|$ =Zero AND $e_n \dot{e}_n$ =Negative THEN δ =Nothing
 IF $e_n \dot{e}_n$ =Positive THEN δ =Large (20)

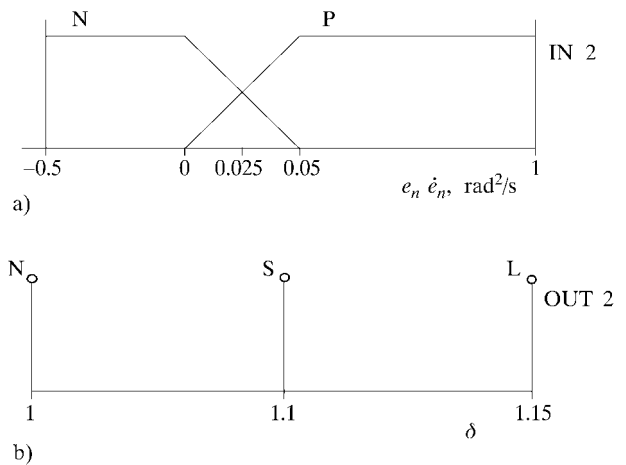


Fig. 6 Membership functions for delta adaptation

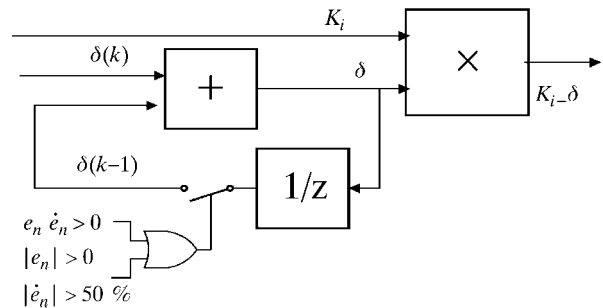


Fig. 7 Principle of delta adaptation

4.1 Tuning of the Supervisory Fuzzy PDF Control

Plant conditions during tuning procedure are as per the nominal values shown in Table 1. Torque reference was limited to 12 N · m. Firstly, the standard PDF controller was tuned, and on the basis of this the adaptive fuzzy supervisor was later adjusted. Taking both the critically damped condition (8) and the stability margins (15) into account, the following values were found to ensure stability:

$$K_i = 56 \text{ Nm/rad for } K_p = 1.89 \text{ Nm} \cdot \text{s/rad}$$

and

$$K_i \text{ Limit} \leq 1350 \text{ Nm/rad.}$$

The absolute normalized error is assigned to input sets in ten-percent steps, as shown in Figure 5. The output membership functions were chosen to obtain the same K_i parameter as the standard PDF controller at regulation (although lower at tracking); the control action was reduced when it was unnecessary. Delta adaptation starts when error evolution is lower than 50 %, and increases K_i step by step as much as the error increases. To prevent instability in the system, the $K_{i-\delta}$ parameter in Figure 7 is limited to 1000 Nm/rad.

5 SIMULATION RESULTS

After adjusting the controllers, several simulations were carried out to determine the effectiveness of the proposed supervisor. The sampling frequency for the simulations was 1 kHz, and the standard Integral of Absolute Error (IAE) index was used to compare controllers' behaviour.

The performance specifications were tested in terms of the transient response for different inputs, such as step, ramp and acceleration input and the S-starting curve, which were computed using Matlab-Simulink. Results are obtained for various cases, and changes in the tuning conditions are indicated for each simulation.

5.1 Step input responses

The response of the controllers to a step input does not involve steady-state errors, and they both show very good responses under a wide range of operating conditions. In fact, as expected, the closer the tuning point, the more similar the response. However, the behaviour of the adaptive controller is most improved when the dynamic of the plant increases, due to additional inputs considered for the supervisor. Figure 8 shows the torque and speed response during starting. Note how the adaptive pro-

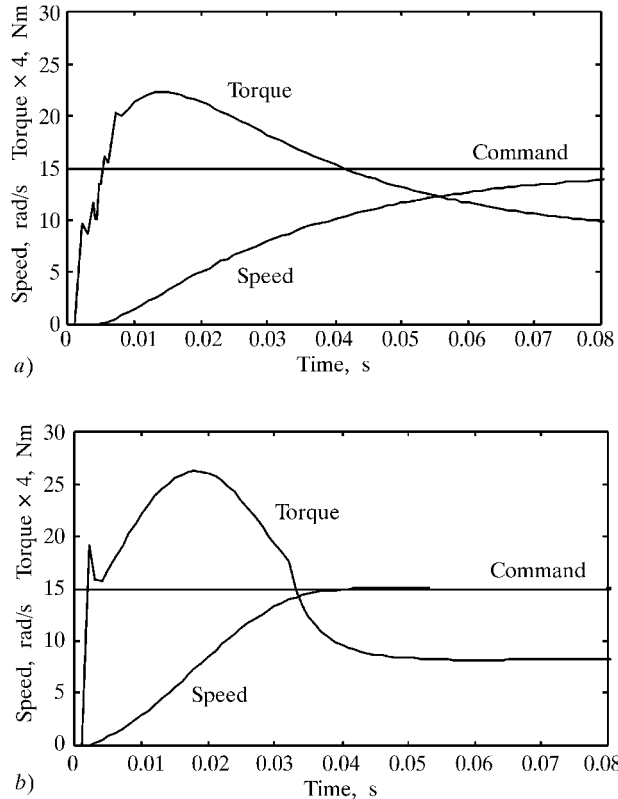


Fig. 8 Step response of the controllers during starting. $J=J_{nom}/1.5$. a) conventional controller; b) adaptive controller

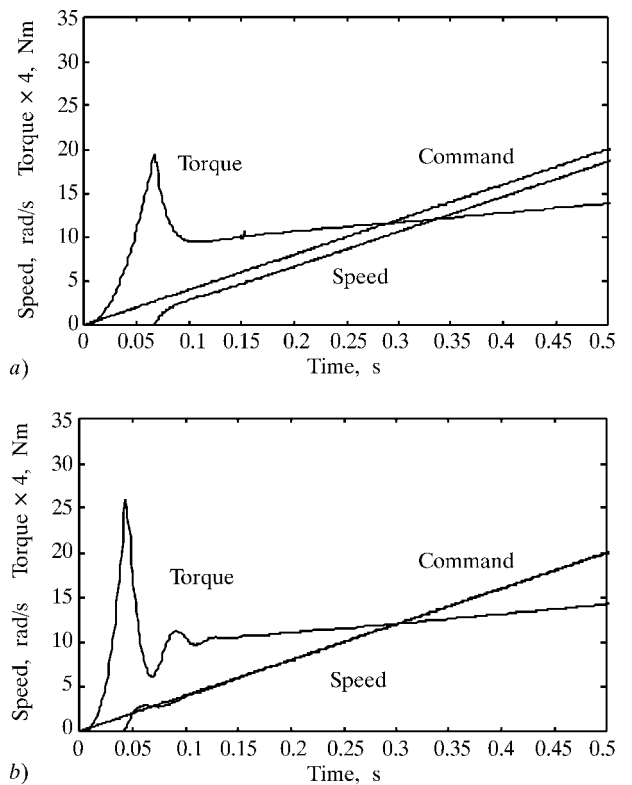


Fig. 9 Ramp tracking responses: starting details. $K_1=K_{1nom} \times 2$. a) conventional controller; b) adaptive controller

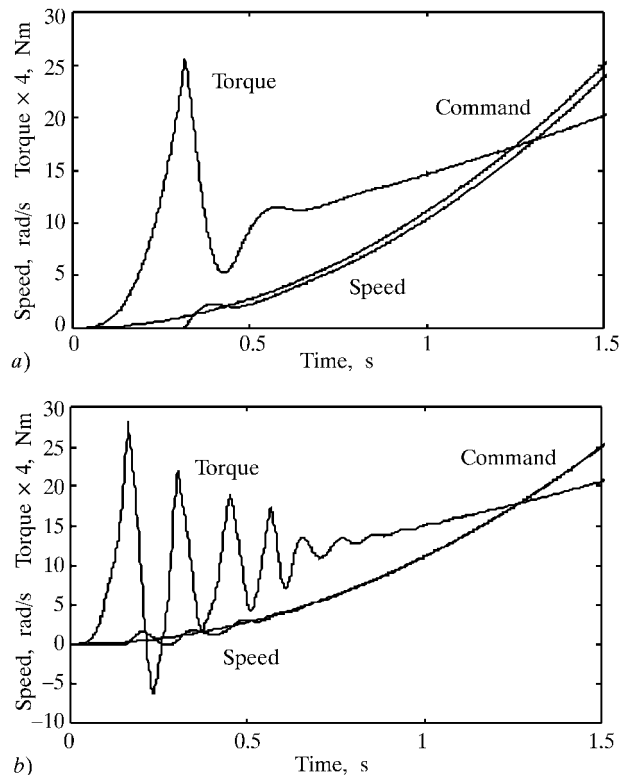


Fig. 10 Parabolic tracking responses: starting details. $J=J_{nom} \times 5$, $K_2=K_{2nom} \times 3$. a) conventional controller; b) adaptive controller

cess increases the control action at start-up, the dynamic error is small, and the drive speed follows the reference speed very closely.

5.2 Ramp input responses

The standard PDF controller is a Type I system, with only one integration on the open-loop transfer function. The steady-state error for a ramp input, which is inversely proportional to the integral constant K_i , cannot be avoided. However, the adaptive controller, which uses both reinforcement action at start-up and delta adaptation later, provides enough control action for a ramp input at starting and quasi-zero actuating error at the steady state to be followed (Figure 9).

The steady-state actuating error of the system with parabolic input (acceleration input) is not constant as in a ramp, but tends towards infinite for a standard PDF controller. It can quite reduced with the adaptive controller, as shown in Figure 10.

However, for a real starting S curve, which is commonplace in industrial drives, the PDF controller is incapable of following the reference input, whereas the adaptive controller can follow it very closely (Figure 11).

The following points can be deduced from the former simulations:

- 1) The performance of the controller proposed is superb in terms of quick torque response, speed overshoot, speed rise time and recovery time.
- 2) No steady-state error occurs under dynamic and static load conditions, even following time-varying references.
- 3) The recovery time is dependent of the adaptive gains of the K_i parameter: the higher the value, the shorter the recovery time, although oscillations may appear.

6 EXPERIMENTAL RESULTS

A laboratory prototype was assembled to verify the features of the control system proposed (Figure 12). The whole drive was based on a multiprocessor system composed of a compatible PC as the host and a DSP auxiliary board PC/32C by Blue-Wave Systems inserted in an ISA bus slot.

The DSP board included a 32-bit-floating-point TMS320C32 processor running at 50 MHz, which interfaced to the host using 2K×16 DPRAM. The board also includes two high-speed I/O expansions, one for four 16-bit analogue input channels, with a maximum sampling rate per channel of 50 kHz, and another for 32 digital I/O lines, seven of which were used to drive the inverter state, gate controls and enable signal. Three analogue channels were used to close the torque control loop, and another to read the mechanical speed.

The task control assignment was distributed between the PC and DSP, so that the first executed algorithms for speed regulation and the second executed algorithms for torque control and space vector modulation to drive the inverter. Moreover, the DSP performed the acquisition and treatment of the analogue plant signals. The DSP also executed the parameter identification algorithms that are needed for vector torque control, though this last loop is not of interest in the discussion of speed regulators carried out in this paper.

The inverter, rated for 220/380 VAC, 50 A, used six power insulated-gate bipolar transistors (IGBTs) driven by a PWM-VSI method, with the necessary drives and protections. The two switches of each leg were driven by complementary signals with some deadtime in order to avoid feedthrough fault. The PWM frequency is 10 kHz, and the sampling time of the speed control loop was 1 ms.

The load of the IM drive is a DC machine working as a generator, loaded with an interchangeable set of resistors to vary load torque. The mechanical characteristic of the shaft of the IM can be modelled using expression (2), where K_1 is made variable depending on the resistor values.

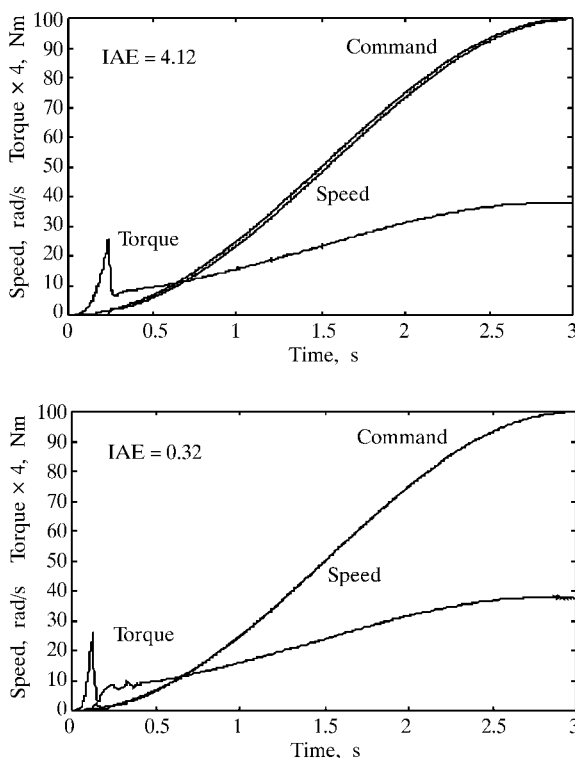


Fig. 11 S-starting response. $J=J_{nom} \times 5$, $K_2=K_{2nom} \times 3$. a) conventional controller; b) adaptive controller

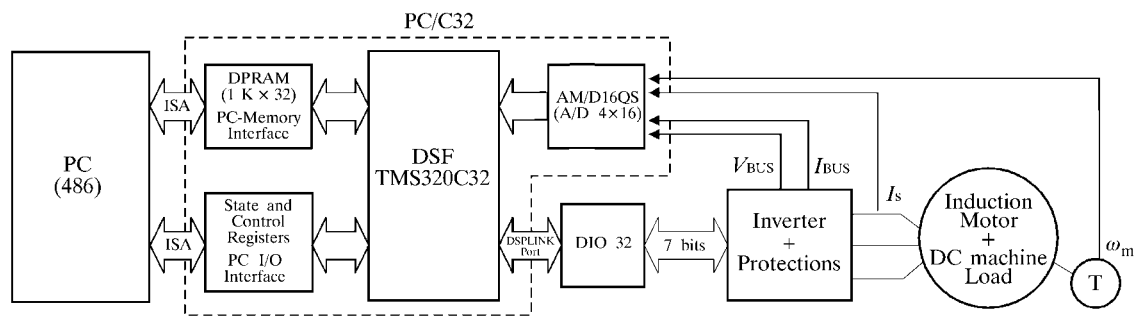


Fig. 12 PC-DSP based experimental setup for IM drive system

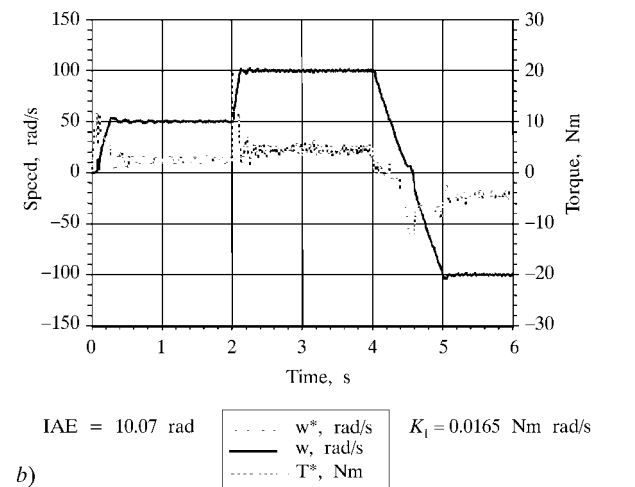
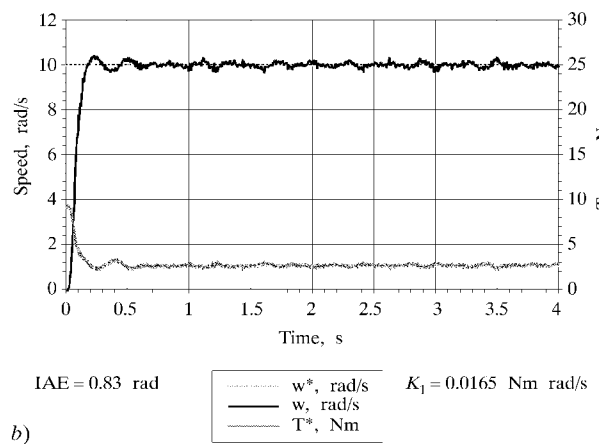
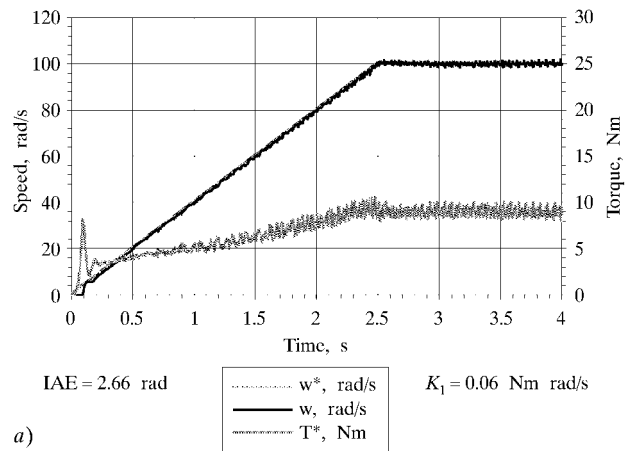
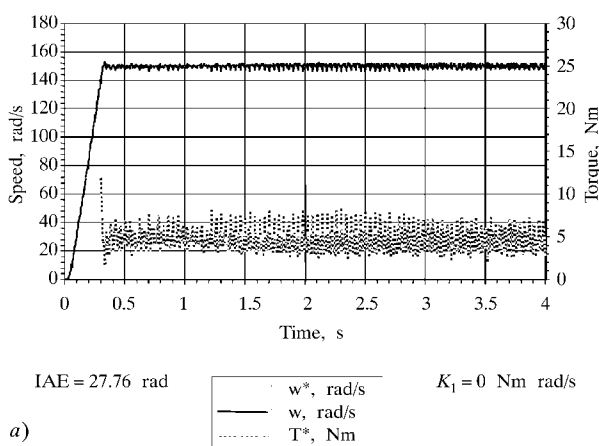


Fig. 13 Experimental responses of the adaptive PDF controller: a) nominal speed reference, b) low speed reference

Fig. 14 Experimental responses of the adaptive PDF controller: a) ramp tracking, b) reversal response

A series of tests were carried out in the experimental setup to verify the proposed scheme under different conditions. The responses to the steps at nominal and low speed reference are depicted in Figure 13, which shows that the motor quickly converges to the reference after start-up, confirming the behaviour expected on the basis of previous simulations.

The ramp tracking and speed reversal response for the motor running at medium load torque are shown in Figure 14. Despite several problems in following the reference near the zero speed, which were probably due to the unsuitable mechanical adjustment of the prototype plant, the adaptive con-

troller followed the input command with very few dynamic or static errors.

The experimental tests point out the effectiveness of the control scheme, and they prove that the adaptation is well reached. The drive response was quite fast, which demonstrates the suitability of the proposed adaptive method for applications in which fast transient response must be maintained.

7 CONCLUSIONS

The theoretical development and practical implementation of adaptive PDF speed control are presented. It was designed with neither a reference model nor recursive estimations, but by defining a self-tuning procedure by means of fuzzy logic. Variable integral action was incorporated through a supervisory adaptation for improving speed response and controlling robustness with respect to command tracking and load variations, which yielded satisfactory drive performance. The simulations and experimental results validated the effectiveness of the suggested regulator. The system rapidly compensated for any output error caused by either variation in the motor's parameters or external torque disturbance, including tracking and regulating states.

We have demonstrated how a very simple fuzzy adaptive system can replace more expansive adaptive PID algorithms for the speed control of an induction motor drive, maintaining the global stability of the system and strongly damped transient states.

ACKNOWLEDGEMENTS

The authors are grateful for the financial support received from the *Spanish Ministry of Science and Technology* as part of the DPI 2001-2213 project.

Neizravno adaptivno upravljanje pogonom s asinkronim motorom. Industrijske primjene sve više trebaju električne pogone s dobrim svojstvima pozicioniranja i regulacije tereta. To se može postići jedino adaptivnim načinom upravljanja, jer se uvjeti terećenja, momenti inercije kao i ostali parametri sustava mijenjaju tijekom gibanja.

U članku je razvijen adaptivni regulator brzine vrtnje za izmjenični pogon s asinkronim motorom koji koristi jednostavan računski algoritam. Autori predlažu samopodešavajuće upravljanje zasnovano na neizravnoj adaptaciji s nadzornog nivoa. Nadzorni algoritam neprestano prati stanje sustava i mijenja parametar K_i standardnog PDF regulatora da bi ga adaptirao na promjene stanja u postrojenju.

Neizravna adaptivna strategija realizirana je bez poteškoća, sa svojstvom vrlo brzog učenja te vrlo dobrim svojstvima pozicioniranja i regulacije tereta. Analiza stabilnosti razvijenog regulatora također je napravljena, a eksperimentalni rezultati pokazuju robustnost predloženog algoritma pri uvjetima djelovanja poremećaja u obliku promjenljivog momenta tereta.

Ključne riječi: adaptivno upravljanje, pogoni podesive brzine vrtnje, neizravna logika, upravljanje gibanjem, pogoni promjenljive brzine vrtnje

AUTHORS' ADDRESSES:

Mohamed Rachid Chekkouri, PhD Student
e-mail: chekkour@eel.upc.es

Dr. Jordi Catal i Lpez, Product Engineer
Control Techniques Iberia SA
e-mail: catala@eel.upc.es

Dr. Emiliano Aldabas Rubira, Lecturer
e-mail: aldabas@eel.upc.es

REFERENCES

- [1] D. Y. Ohm, **Analysis of PID and PDF Compensators for Motion Control Systems**. Report on the 1994 IEEE Industry Applications Conference Society Meeting, vol. 3, pp. 1923–1929, Denver, USA, Oct. 1994.
- [2] S. Weerasooriya, M. A. El-Sharkawi, **Adaptive Tracking Control for High Performance dc Drives**. IEEE Transaction on Energy Conversion, vol. 4, no. 3, pp. 502–508, Sept. 1989.
- [3] E. Cerruto, A. Consoli, A. Raciti, A. Testa, **Fuzzy Adaptive Vector Control of Induction Motors Drives**. IEEE Trans. on Power Electronics, vol. 12, no. 2, pp. 1028–1040, Nov. 1997.
- [4] W. Khan, D. Taylor, **Adaptive Control of ac Motor Drives with Inverter Non-linearities**. International Journal of Control, vol. 72, pp. 784–798, 1999.
- [5] M.-F. Tsai, Y.-Y. Tzou, **A Transputer-Based Adaptive Speed Controller for AC Induction Motor Drives with Load Torque Estimation**. IEEE Transactions on Industry Applications, vol. 33, no. 2, pp. 558–566, March–April 1997.
- [6] T. J. Kweon, D. S. Hyun, **High Performance Speed Control of Electric Machines Using the Kalman Filter and Self-tuning Regulator**. Conference Record of the 1998 IEEE Power Electronics Specialist Conference, PESC'98, vol. 1, pp. 280–286, Fukuoka, Japan, May 1998.
- [7] A. Suyitno, J. Fujikawa, H. Kobayashi, Y. Dote, **Variable-Structured Robust Controller by Fuzzy Logic for Servomotors**. IEEE Transactions on Industrial Electronics, vol. 40, pp. 80–88, February 1993.
- [8] Y. Dote, M. Strefezza, A. Suyitno, **Variable-Structured Robust Control by Fuzzy Logic and Stability Analysis for an AC Drive System**. Proceedings of the International Conference on Industrial Electronics, Control and Instrumentation, IECON'93, vol. 3, pp. 1962–1967, Maui Hawaii, USA, Nov. 1993.
- [9] G. Ellis, R. D. Lorenz, **Comparison of Motion Control Loops for Industrial Applications**. Report on the 1999 IEEE Industry Applications Conference, Thirty-Fourth IAS Annual Meeting, vol. 4, pp. 2599–2605, Phoenix, USA, Oct. 1999.
- [10] K. Ogata, **Modern Control Engineering**. Prentice-Hall, Inc., 1970.

Dr. Luis Romeral Martínez, Senior Lecturer
e-mail: romeral@eel.upc.es

Electronic Engineering Department
Technical University of Catalonia
Campus Terrassa, TR2. C/Colom, no. 1
08222. Terrassa, Catalonia, Spain.
Phone number: +34 93 739 8194
Fax number: +34 93 739 8016

Received: 2003–11–14